Testing the electroweak phase transition and electroweak baryogenesis at LHC and a circular electron-positron collider

Fa Peng Huang*,[1] Pei-Hong Gu,[2] Peng-Fei Yin,[3] Zhao-Huan Yu,[3,4] and Xinmin Zhang[1]

[1] *Theoretical Physics Division, Institute of High Energy Physics, Chinese Academy of Sciences, P.O.Box 918-4, Beijing 100049, P.R.China*

[2] *Department of Physics and Astronomy, Shanghai Jiao Tong University, 800 Dongchuan Road, Shanghai 200240, China*

[3] *Key Laboratory of Particle Astrophysics, Institute of High Energy Physics, Chinese Academy of Science, P.O.Box 918-3, Beijing 100049, P. R. China*

[4] *ARC Centre of Excellence for Particle Physics at the Terascale, School of Physics, The University of Melbourne, Victoria 3010, Australia*

arXiv:1511.03969v3 [hep-ph] 17 May 2016

We study the collider phenomenology of the electroweak phase transition and electroweak baryogenesis in the framework of the effective field theory. Our study shows that the effective theory using the dimension-6 operators can enforce strong first order phase transition and provide sizable CP violation to realize a successful electroweak baryogenesis. Such dimension-6 operators can induce interesting Higgs phenomenology that can be verified at colliders such as the LHC and the planning CEPC. We then demonstrate that this effective theory can originate from vector-like quarks and the triplet Higgs.

PACS numbers: 98.80.Cq,12.60.-i

I. INTRODUCTION

A longstanding problem in particle physics and cosmology is to unravel the origin of baryon asymmetry of the universe (BAU), which is quantified by the baryon-to-photon ratio $\eta = n_B/n_\gamma = 6.05(7) \times 10^{-10}$ [1, 2]. The current value η is obtained from investigations of the big bang nucleosynthesis or the power spectrum of the cosmic microwave background radiation. To generate the BAU (baryogenesis), it needs three necessary conditions, i.e. baryon number violation, C and CP violation, and departure from equilibrium dynamics or CPT violation [3]. To satisfy the three conditions for baryogenesis, many possible mechanisms, such as Planck-scale baryogenesis, GUT baryogenesis, Affleck-Dine baryogenesis, leptogenesis, and electroweak (EW) baryogenesis have been proposed [4], but after the discovery of the 125 GeV Higgs boson [5, 6] at the LHC, EW baryogenesis [7, 8] becomes a popular and testable scenario for explaining the BAU [9], wherein the BAU is driven by the EW sphaleron (baryon number violation) and the generation of CP asymmetry (C and CP violation) at the time of the EW phase transition (departure from equilibrium dynamics). For efficient production of BAU, a strong first order phase transition (SFOPT) and sizable CP violation are necessary. However, in the standard model (SM), the 125 GeV Higgs boson is too heavy for a SFOPT [9], and the CP violation from CKM matrix is too weak.

Another urgent problem in particle physics after the discovery of the Higgs boson is to explore the true shape of the Higgs potential, the nature of the EW spontaneous symmetry breaking, and the type of the EW phase transition. However, the current experiments at the LHC only provide us with a rough picture of these problems. For the Higgs potential, we know nothing but the quadratic oscillation around the vacuum expectation value (vev) v with the 125 GeV mass. Understanding these problems can also help to understand the above EW baryogenesis problem.

To provide both the SFOPT and sizable CP violation for EW baryogenesis, we follow the effective field theory (EFT) approach in Refs. [10–14]) to realize the EW baryogenesis by introducing dimension-6 operators $-x_u^{ij}\frac{\phi^\dagger\phi}{\Lambda^2}\bar{q}_{Li}\tilde{\phi}u_{Rj} + \text{H.c.} - \frac{\kappa}{\Lambda^2}(\phi^\dagger\phi)^3$ in this paper. The dimension-6 operators will modify the shape of the Higgs potential and yield distinctive signals at the LHC, such as the different Higgs pair production behavior. Due to experimental precision of the LHC, LHC may only give some hints and be difficult to precisely test this type of EW baryogenesis scenario. However, the Circular Electron-Positron Collider (CEPC)[15] has the ability to precisely test this type of the EW phase transition and the EW baryogenesis, which is the main goal of the CEPC. Detailed discussions on testing the EW phase transition and the EW baryogenesis will be given in the following. For completeness, a renormalizable extension model is given to obtain the needed dimension-6 operators for the EW baryogenesis.

In Sec. II, we describe the effective operators in the EFT framework, and show that the dimension-6 operators can change the Higgs potential, realize the SFOPT, and provide the CP violation source for the EW baryogenesis. In

* Electronic address: huangfp@ihep.ac.cn

Sec. III, we discuss the collider phenomenology of this EW baryogenesis scenario induced by the dimension-6 operators at the LHC and the future CEPC, especially the Higgs phenomenology. In Sec. IV, the possible renormalizable model is given. Finally, we conclude in Sec. V.

II. AN EFFECTIVE THEORY FOR EW BARYOGENESIS

In this paper, the EFT approach is adopted to provide the needed SFOPT and CP violation for the EW baryogenesis. This allows us to derive model-independent predictions and constraints on the EW baryogenesis using the following effective operators:

$$\mathcal{L}_{\rm eff} = \mathcal{L}_{\rm SM} + \Sigma_i \frac{1}{\Lambda^{d_i-4}} \kappa_i \mathcal{O}_i, \tag{1}$$

where d_i are the dimensions of the new operators, and $\mathcal{O}_i$ are invariant under the SM gauge symmetry and contain only the SM fields. The parameters κ_i is the Wilson coefficient, which can be determined by matching the full theory to the effective operators. Λ is the cutoff energy scale, at which the effective theory breaks down.

A. The effective Lagrangian

In addition to the relevant Lagrangian of the Higgs sector in the SM

$$\mathcal{L}_{\rm SM} \supset -y_u^{ij} \bar{q}_{Li} \tilde{\phi} u_{Rj} + \text{H.c.} - \mu^2 \phi^\dagger \phi - \lambda (\phi^\dagger \phi)^2 \,, \tag{2}$$

we commence our study on the EW baryogenesis from the effective Lagrangian with the following dimension-6 operators [10–14]:

$$\delta\mathcal{L} = -x_u^{ij} \frac{\phi^\dagger \phi}{\Lambda^2} \bar{q}_{Li} \tilde{\phi} u_{Rj} + \text{H.c.} - \frac{\kappa}{\Lambda^2} (\phi^\dagger \phi)^3 \,, \tag{3}$$

where ϕ is the Higgs doublet field and $\tilde{\phi} = i\tau_2 \phi^*$. q_L and u_R are the left-handed quarks and the right-handed up-type quarks, respectively. Thus,

$$\phi(1,2,-\tfrac{1}{2}) = \begin{bmatrix} \phi^0 \\ \phi^- \end{bmatrix}, \quad q_L(3,2,+\tfrac{1}{6}) = \begin{bmatrix} u_L \\ d_L \end{bmatrix}, \quad u_R(3,1,+\tfrac{2}{3}) \,. \tag{4}$$

Here and hereafter the brackets following the fields describe the transformations under the $SU(3)_c \times SU(2)_L \times U(1)_Y$ gauge group. The effective Lagrangian in Eq. (3) can be obtained in many models beyond the SM, such as some strong dynamics models. In Sec. IV, a renormalizable model is given. The early study of the SFOPT using the $(\phi^\dagger\phi)^3$ effective opertor was first given in Ref. [10], and the recent studies can be found in Refs. [16–23].

B. SFOPT and the true Higgs potential

From Eqs. (2) and (3), the potential of the Higgs boson field can be written as

$$V(\phi) = \mu^2 \phi^\dagger \phi + \lambda (\phi^\dagger \phi)^2 + \frac{\kappa (\phi^\dagger \phi)^3}{\Lambda^2}. \tag{5}$$

By introducing the non-renormalizable term $(\phi^\dagger\phi)^3$ in the potential, the SFOPT may be realized. When the SFOPT is considered, we can simplify the potential by substituting ϕ with $h/\sqrt{2}$:

$$V_{\rm tree}(h) = \frac{1}{2}\mu^2 h^2 + \frac{\lambda}{4} h^4 + \frac{\kappa}{8\Lambda^2} h^6. \tag{6}$$

Using the methods in Refs. [24, 25], the full finite-temperature effective potential up to one-loop level is composed of three parts,

$$V_{\rm eff}(h,T) = V_{\rm tree}(h) + V_1^{T=0}(h) + \Delta V_1^{T\neq 0}(h,T), \tag{7}$$

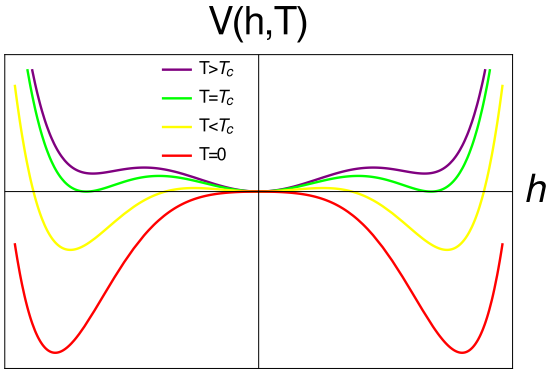

FIG. 1: The schematic diagram of the Higgs potential for SFOPT at different temperatures.

where $V_{\rm tree}(h)$ is the tree-level potential, $V_1^{T=0}(h)$ is the Coleman-Weinberg potential at zero temperature, and $\Delta V_1^{T\neq 0}(h)$ is the leading thermal correction including the daisy resummation. However, in this scenario, the dominant contribution for the SFOPT comes from the tree level barrier as shown in Fig. 1, and thus the effective potential with finite temperature effects can be approximated as

$$V_{\rm eff}(h,T) \approx \frac{1}{2}\left(\mu^2 + c\,T^2\right)h^2 + \frac{\lambda}{4}h^4 + \frac{\kappa}{8\Lambda^2}h^6. \tag{8}$$

The finite temperature effects are included in the coefficient c of the thermal mass with

$$c = \frac{1}{16}(g'^2 + 3g^2 + 4y_t^2 + 4\frac{m_h^2}{v^2} - 12\frac{\kappa v^2}{\Lambda^2}), \tag{9}$$

where g and g' are the $SU(2)_L$ and $U(1)_Y$ gauge couplings, and y_t is the top quark Yukawa coupling in the SM. To keep the observed Higgs boson mass $m_h = 125$ GeV and the vev v , λ and μ^2 should be changed as

$$\lambda = \frac{m_h^2}{2v^2}\left(1 - \frac{\Lambda_{\rm max}^2}{\Lambda^2}\right), \tag{10}$$

$$\mu^2 = \frac{m_h^2}{2}\left(-1 + \frac{\Lambda_{\rm max}^2}{2\Lambda^2}\right), \tag{11}$$

with $\tilde{\Lambda}_{\rm max} \equiv \sqrt{3\kappa}v^2/m_h$. In the limit $\Lambda \to \infty$, λ and μ^2 are recovered to the SM cases as

$$\lambda(\Lambda \to \infty) = \frac{m_h^2}{2v^2}, \tag{12}$$

$$\mu^2(\Lambda \to \infty) = -\frac{m_h^2}{2}. \tag{13}$$

The Higgs potential in Eq. (6) could trigger the desired spontaneous symmetry breaking as in the SM. To realize the SFOPT, it needs $\mu^2 + c\,T^2 > 0$ to make the EW-symmetric vacuum stable, $\lambda < 0$ to reverse the potential, and the h^6 term to stabilize the EW-broken vacuum as shown in Fig. 1. In order to guarantee the SFOPT, λ must be negative under the above approximation, and thus, from Eq. (10), we obtain an upper bound on Λ, namely $\Lambda < \tilde{\Lambda}_{\rm max} \approx 840\sqrt{\kappa}$ GeV. From the requirements of perturbativity, $\kappa < 4\pi$. If we choose a larger κ, we can get a larger upper bound $\tilde{\Lambda}_{\rm max}$. For example, if $\kappa = 12.5$, then $\tilde{\Lambda}_{\rm max} = 3$ TeV. This large upper bound leaves large space to discuss the phenomenology at the 14 TeV LHC.

Using the standard techniques in the study of the EW baryogenesis, we obtain the phase transition critical temperature T_c and the washout parameter $v(T_c)/T_c$ as the following:

$$T_c = \frac{\sqrt{\lambda^2\Lambda^2 - 4\kappa\mu^2}}{2\sqrt{c\kappa}}, \tag{14}$$

$$\frac{v(T_c)}{T_c} = \frac{2\Lambda\sqrt{-c\lambda}}{\sqrt{\lambda^2\Lambda^2 - 4\kappa\mu^2}}. \tag{15}$$

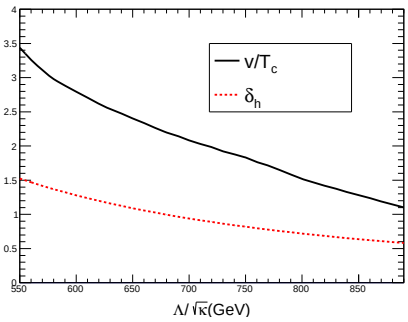

FIG. 2: The dependence of the washout parameter and the modification of the trilinear Higgs boson coupling on $\Lambda/\sqrt{\kappa}$.

$T_c > 0$ gives a lower bound $\tilde{\Lambda}_{\rm min} \equiv \tilde{\Lambda}_{\rm max}/\sqrt{3} = \sqrt{\kappa}v^2/m_h$. For $m_h = 125$ GeV, this gives $\tilde{\Lambda}_{\rm min} \approx 480\sqrt{\kappa}$ GeV.

After including the full one-loop results as given in Refs. [17, 21], the dependence of the washout parameter on $\Lambda/\sqrt{\kappa}$ is shown in Fig. 2, and it shows that the washout condition for the SFOPT,

$$\frac{v(T_c)}{T_c} \gtrsim 1, \tag{16}$$

can be easily satisfied roughly from 550 to 890 GeV. For instance, taking $\Lambda/\sqrt{\kappa} = 620$ GeV, the washout parameter $v/T_c = 2.6$ for the full one-loop case and $v/T_c = 2.8$ for the leading thermal approximation case. It is worth noticing that for $\Lambda/\sqrt{\kappa} \lesssim 550$ GeV, the phase transition will not occur by the "metastability" [21] and for $\Lambda/\sqrt{\kappa} > 840$ GeV, the parameter λ becomes positive. Thus, after considering the full one-loop results and the metastability, the allowed range changes from the approximation result 480 GeV $< \Lambda/\sqrt{\kappa} <$ 840 GeV to roughly 550 GeV $\lesssim \Lambda/\sqrt{\kappa} \lesssim$ 890 GeV.

An interesting consequence is that the requirement of the SFOPT would lead to obvious modification of the trilinear Higgs boson coupling as

$$\mathcal{L}_{hhh} = -\frac{1}{3!}(1+\delta_h)A_h h^3, \tag{17}$$

where $A_h = 3m_h^2/v$ is the trilinear Higgs boson coupling in the SM, and δ_h is the modification of the trilinear Higgs coupling induced by the dimension-6 operator. In this scenario, δ_h roughly varies from 0.6 to 1.5 in the allowed parameter space as shown in Fig. 2. Hints of the large deviation of the trilinear Higgs coupling may be seen at the 14 TeV LHC, and its precise probe may be obtained in the future CEPC [26–28], which will be discussed in details below.

C. CP violation source

Besides the SFOPT, the BAU also needs sizable source of CP violation, which can be provided by the dimension-6 operator $-x_u^{ij}\frac{\phi^\dagger\phi}{\Lambda^2}\bar{q}_{Li}\tilde{\phi}u_{Rj} + \text{H.c.}$ in Eq. (3). For simplicity, only the top quark is considered in this paper. Therefore, this effective operator can induce the anomalous top quark Yukawa coupling $\frac{v^2}{2\Lambda^2}h[\text{Re}(x_u^{ij})\bar{t}t + i\,\text{Im}(x_u^{ij})\bar{t}\gamma^5 t]$. For simplicity, we denote $\text{Re}(x_u^{33}) = a$ and $\text{Im}(x_u^{33}) = b$. Then the CP violation source from Eq. (3) can be rewritten as

$$\frac{v^2}{2\Lambda^2}h(a\bar{t}t + ib\bar{t}\gamma^5 t). \tag{18}$$

To avoid the non-minimal flavour violation [29, 30], we assume that $x_u^{ij} = 0$ except for $x_u^{33} \neq 0$. Hence, the Lagrangian for the effective interaction between the top quark and the Higgs boson is parameterized as

$$\mathcal{L} = -\frac{m_t}{v}h\bar{t}(1+\delta_t^+ + i\delta_t^-\gamma^5)t, \tag{19}$$

with

$$\delta_t^+ = \frac{av^3}{2\Lambda^2 m_t}, \tag{20}$$

and

$$\delta_t^- = \frac{bv^3}{2\Lambda^2 m_t}. \tag{21}$$

The $i\gamma^5$ term is CP-odd, and would provide the CP violation source for the EW baryogenesis. And thus, the top quark acquires a complex mass inside the bubble walls, which is expressed as [31, 32]

$$m_t(z) = \frac{m_t}{v}(1 + \delta_t^+ + i\delta_t^-\gamma^5)h(z) \equiv |m_t(z)|e^{i\Theta(z)}. \tag{22}$$

Here, z is just the coordinate transverse to the bubble wall, and Θ is the CP violation phase. Using the approximate method with the more recent and complete transport equations in Refs. [32–34], the baryon asymmetry is given by[1]

$$\eta_B = \frac{405\Gamma_{\rm sph}}{4\pi^2 v_{\rm wall} g_* T}\int dz\, \mu_{B_L} f_{\rm sph}\, e^{-45\,\Gamma_{\rm sph}|z|/(4v_{\rm wall})}, \tag{23}$$

which depends on the sphaleron washout parameter v_c/T_c, the bubble wall velocity $v_{\rm wall}$, the bubble wall thickness $L_{\rm wall}$, and so on. Here, $f_{\rm sph} \approx \min(1, 2.4{\rm T}/\Gamma_{\rm sph}{\rm e}^{-40{\rm v}/{\rm T}})$. Preliminary numerical estimation gives a rough estimation on the anomalous top quark Yukawa coupling as

$$\delta_t^- = \mathcal{O}(0.01 - 1)\,, \tag{24}$$

which can provide sizable CP violation source for a successful EW baryogenesis. Due to the fact that the exact calculations of the baryon asymmetry η_B rely on the improvements of the non-perturbative dynamics, such as the bubble wall dynamics, we can only obtain a rough constraint on the anomalous top quark Yukawa coupling from η_B and we will discuss how to constrain the anomalous coupling from experiments in particle physics, where more accurate constraints might be obtained.

III. COLLIDER PHENOMENOLOGY FROM THE LHC TO THE CEPC

From the above discussions on the EW baryogenesis induced by the dimension-6 operators in Eq. (3), we see that the realization of the EW baryogenesis will lead to obvious modifications of the trilinear Higgs boson coupling and the top quark Yukawa coupling on the SM values, which may leave hints at the 14 TeV LHC, and further be precisely tested at the future CEPC. The deviations due to Eq. (3) can be written as

$$-\mathcal{L} = \frac{1}{3!}\left(\frac{3m_h^2}{v}\right)(1+\delta_h)\,h^3 \;+\; \frac{m_t}{v}h\bar{t}(1 + \delta_t^+ + i\delta_t^-\gamma^5)t\,. \tag{25}$$

In the SM, $\delta_h = \delta_t^+ = \delta_t^- = 0$.

A. Collider phenomenology at the LHC

Now, we discuss the constraints and possible signals of the anomalous couplings δ_h, δ_t^+, and δ_t^- at the LHC. Firstly, we consider the phenomenology of the anomalous top quark Yukawa coupling.

In low energy experiments, the CP-odd top Yukawa coupling is constrained from the electron electric dipole moments (EDM), neutron EDM, and Hg EDM, etc taking into account all uncertainties in the low energy matrix elements[13, 35–39]. Among these low energy experiments, the electron EDM give the strong constraints $\delta_t^- < \mathcal{O}(0.01)$, but depends on the so far not measured SM electron Yukawa coupling. Introducing new baryogenesis unrelated CP violation source [40, 41] or modifying the electron Yukawa coupling can relax the stringent constraints from the electron EDM. The neutron EDM does not suffer from the electron Yukawa coupling (it can be induced purely from the interaction

[1] The expressions of the baryon asymmetry in Refs. [32, 34] are based on the more recent result in Ref. [33], which improves the result in Ref. [21] with the more recent and complete transport equations. The baryon asymmetry expression in Ref. [33] is obtained in the wall frame. In this work, we focus on the study of the collider phenomenology rather than the transport details, which are given in Refs. [21, 33].

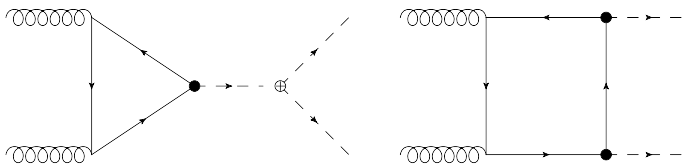

FIG. 3: The sample leading order Feynman diagrams for the Higgs boson pair production induced by the top quark loop at the 14 TeV LHC.

of the top quark and Higgs boson) and its bound, including all uncertainties, roughly gives $\delta_t^- < \mathcal{O}(0.1)$, which still leaves room for successful baryogenesis. The Hg EDM gives no constraints anymore after the uncertainties are taken into account. Detailed discussion on the cancellations between the EDM with a CP violation Higgs sector can be found in Ref. [30]. In the following discussions, we assume that the constraints from the EDMs are relaxed and investigate the collider constraints.

The modifications of the anomalous top quark Yukawa coupling would also affect the single Higgs production $gg \to h$ and the Higgs pair production $gg \to hh$ via gluon fusions and the Higgs decay to photons $h \to \gamma\gamma$ at hadron colliders. It is possible to constrain the deviations to be of $\mathcal{O}(0.1)$ at the LHC [42]. The anomalous top quark Yukawa coupling would modify the Higgs couplings to gg and $\gamma\gamma$. The loop induced Higgs couplings g_{hgg} and $g_{h\gamma\gamma}$ can be parameterized as [42–44]

$$g^2_{hgg}/g^2_{hgg,\mathrm{SM}} \simeq (1+\delta_t^+)^2 + 0.11\delta_t^+(1+\delta_t^+) + 2.6(\delta_t^-)^2, \tag{26}$$

$$g^2_{h\gamma\gamma}/g^2_{h\gamma\gamma,\mathrm{SM}} \simeq (1-0.28\delta_t^+)^2 + (0.43\delta_t^-)^2. \tag{27}$$

Unlike the associated Higgs production, both CP-even and CP-odd top quark Yukawa couplings enter the Higgs decays to gg and $\gamma\gamma$. It can be seen that δ_t^- has important contribution to g_{hgg} from Eq. (26). The numerical constraints will be discussed in the subsection of CEPC below.

Meanwhile, these three deviations will modify the behavior of the Higgs boson pair production at the LHC. The sample Feynman diagrams for the Higgs boson pair production are shown in Fig. 3. The kinematic invariants are defined as $\hat{s} = (p_a + p_b)^2$, $\hat{t} = (p_a + p_c)^2$, and $\hat{u} = (p_b + p_c)^2$ with $p_a + p_b + p_c + p_d = 0$. And we also define the following kinematic variables:

$$\mathcal{S} = \hat{s}/m_t^2, \quad \mathcal{T} = \hat{t}/m_t^2, \quad \mathcal{U} = \hat{u}/m_t^2, \quad \rho_c = m_h^2/m_t^2, \quad \mathcal{T}_1 = \mathcal{T} - \rho_c, \quad \mathcal{U}_1 = \mathcal{U} - \rho_c, \quad \mathcal{P}(\hat{s}) = \frac{3m_h^2}{\hat{s} - m_h^2 + im_h\Gamma_h}.$$

Using `FeynCalc` [45], the partonic differential cross section for the $g(p_a)g(p_b) \to h(p_c)h(p_d)$ process can be obtained as

$$\begin{aligned}
\frac{d\hat{\sigma}(gg \to hh)}{d\hat{t}} &= \frac{G_F^2\alpha_s^2}{512(2\pi)^3}\Big\{\Big|(1+\delta_h)(1+\delta_t^+)\mathcal{P}(\hat{s})F_\triangle^A + (1+\delta_t^+)^2F_\square^{AA} + (\delta_t^-)^2F_\square^{BB}\Big|^2 \\
&+ \Big|(1+\delta_t^+)\delta_t^-G_\square^{AB}\Big|^2 + \Big|(1+\delta_t^+)^2G_\square^{AA} + (\delta_t^-)^2G_\square^{BB}\Big|^2 \\
&+ \Big|(1+\delta_h)\delta_t^-\mathcal{P}(\hat{s})F_\triangle^B + (1+\delta_t^+)\delta_t^-F_\square^{AB}\Big|^2\Big\},
\end{aligned} \tag{28}$$

where $F_\triangle^A$, $F_\square^{AA}$, $F_\square^{BB}$, $F_\triangle^B$, $F_\square^{AB}$, and $G_\square^{AA}$ are the corresponding form factors:

$$F_\triangle^A = \frac{2}{\mathcal{S}}\left\{2 + (4-\mathcal{S})m_t^2C_{ab}\right\}, \tag{29}$$

$$\begin{aligned}
F_\square^{AA} &= \frac{1}{\mathcal{S}^2}(4S + 8\mathcal{S}m_t^2C_{ab} - 2\mathcal{S}(\mathcal{S}+2\rho_c-8)m_t^4(D_{abc}+D_{bac}+D_{acb}) \\
&+ (2\rho_c-8)m_t^2(\mathcal{T}_1C_{ac} + \mathcal{U}_1C_{bc} + \mathcal{U}_1C_{ad} + \mathcal{T}_1C_{bd} - (\mathcal{T}\mathcal{U} - \rho_c^2)m_t^2D_{acb})),
\end{aligned} \tag{30}$$

$$G_\square^{AA} = \frac{1}{\mathcal{S}(\mathcal{T}\mathcal{U} - \rho_c^2)}((\mathcal{T}^2 + \rho_c^2 - 8\mathcal{T})m_t^2(\mathcal{S}C_{ab} + \mathcal{T}_1C_{ac} + \mathcal{T}_1C_{bd} - \mathcal{S}\mathcal{T}m_t^2D_{bac})$$

$$
\begin{aligned}
&+ (\mathcal{U}^2+\rho_c^2-8\mathcal{U})m_t^2(\mathcal{S}C_{ab}+\mathcal{U}_1C_{bc}+\mathcal{U}_1C_{ad}-\mathcal{S}\mathcal{U}m_t^2D_{abc})\\
&- (\mathcal{T}^2+\mathcal{U}^2-2\rho_c^2)(\mathcal{T}+\mathcal{U}-8)m_t^2C_{cd}\\
&- 2(\mathcal{T}+\mathcal{U}-8)(\mathcal{T}\mathcal{U}-\rho_c^2)m_t^4(D_{abc}+D_{bac}+D_{acb})),
\end{aligned}
\tag{31}
$$

$$
F_{\triangle}^{B}=-2m_t^2C_{ab},
\tag{32}
$$

$$
F_{\square}^{AB}=-2m_t^4(D_{abc}+D_{bac}+D_{acb}),
\tag{33}
$$

$$
\begin{aligned}
G_{\square}^{AB} &= \frac{1}{\mathcal{S}(\mathcal{T}\mathcal{U}-\rho_c^2)}((\mathcal{U}^2-\rho_c^2)m_t^2(\mathcal{S}C_{ab}+\mathcal{U}_1C_{bc}+\mathcal{U}_1C_{ad}-\mathcal{S}\mathcal{U}m_t^2D_{abc})\\
&- (\mathcal{T}^2-\rho_c^2)m_t^2(\mathcal{S}C_{ab}+\mathcal{T}_1C_{ac}+\mathcal{T}_1C_{bd}-\mathcal{S}\mathcal{T}m_t^2D_{bac})\\
&+ ((\mathcal{T}+\mathcal{U})^2-4\rho_c^2)(\mathcal{T}-\mathcal{U})m_t^2C_{cd}\\
&+ 2(\mathcal{T}-\mathcal{U})(\mathcal{T}\mathcal{U}-\rho_c^2)m_t^4(D_{abc}+D_{bac}+D_{acb})),
\end{aligned}
\tag{34}
$$

$$
\begin{aligned}
F_{\square}^{BB} &= \frac{1}{\mathcal{S}^2}(4\mathcal{S}+8\mathcal{S}m_t^2C_{ab}-2\mathcal{S}(\mathcal{T}+\mathcal{U})m_t^4(D_{abc}+D_{bac}+D_{acb})\\
&+ 2\rho_cm_t^2(\mathcal{T}_1C_{ac}+\mathcal{U}_1C_{bc}+\mathcal{U}_1C_{ad}+\mathcal{T}_1C_{bd}-(\mathcal{T}\mathcal{U}-\rho_c^2)m_t^2D_{acb})),
\end{aligned}
\tag{35}
$$

$$
\begin{aligned}
G_{\square}^{BB} &= \frac{1}{\mathcal{S}(\mathcal{T}\mathcal{U}-\rho_c^2)}((\mathcal{T}^2+\rho_c^2)m_t^2(\mathcal{S}C_{ab}+\mathcal{T}_1C_{ac}+\mathcal{T}_1C_{bd}-\mathcal{S}\mathcal{T}m_t^2D_{bac})\\
&+ (\mathcal{U}^2+\rho_c^2)m_t^2(\mathcal{S}C_{ab}+\mathcal{U}_1C_{bc}+\mathcal{U}_1C_{ad}-\mathcal{S}\mathcal{U}m_t^2D_{abc})\\
&- (\mathcal{T}^2+\mathcal{U}^2-2\rho_c^2)(\mathcal{T}+\mathcal{U})m_t^2C_{cd}\\
&- 2(\mathcal{T}+\mathcal{U})(\mathcal{T}\mathcal{U}-\rho_c^2)m_t^4(D_{abc}+D_{bac}+D_{acb})).
\end{aligned}
\tag{36}
$$

The definitions of the scalar integrals C_{ij} and D_{ijk} can be found in the appendix. In the case of $\delta_t^+=\delta_t^-=0$, there has been extensive study on extracting the δ_h from LHC data [46–55]. If we further let $\delta_h=0$, the differential cross section here can reduce to the SM case as in Refs. [56, 57].

The cross section of the Higgs boson pair production depends on all the three anomalous couplings δ_h, δ_t^+, and δ_t^-, which are all related to the energy cutoff Λ. By convoluting the partonic cross section in Eq. (28) with the parton distribution function $G(x,\mu_f)_{g/P}$, the differential cross section at hadron level becomes

$$
\sigma(PP\to hh)=\int dx_adx_bG(x_a,\mu_f)_{g/P}G(x_b,\mu_f)_{g/P}\hat{\sigma}(gg\to hh).
\tag{37}
$$

The numerical results of the normalized invariant mass distributions for the Higgs boson pair are shown in Fig. 4, which is very different from the SM case for the sample points $\delta_h=1,\delta_t^+=0,\delta_t^-=0.1$ and $\delta_h=1,\delta_t^+=0,\delta_t^-=0$. In the SM, it only has one peak located at about 400 GeV. But in this EW baryogenesis scenario, it has two peaks, one peak located at about 260 GeV, and the other one located at about 420 GeV. This character of the invariant mass distribution of the Higgs boson pair can be used to test this EW baryogenesis scenario induced by the dimension-6 operators. Due to the difficulties to suppress the backgrounds at the hadron colliders, it will be difficult to completely pin down these anomalous couplings at the 14 TeV LHC, even with 3000 fb^{-1} integrated luminosity. Exploiting the boosted tricks may help to increase the ability to extract the anomalous coupling. More precise constraints may come from the future CEPC experiments.

B. Collider phenomenology at the CEPC

Further, we discuss how to precisely test this EW phase transition and EW baryogenesis scenario at the CEPC, where the measurements are of great precision.

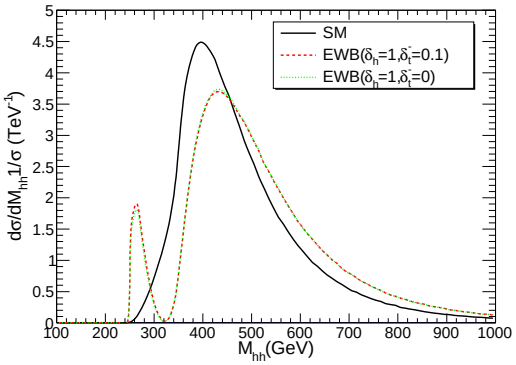

FIG. 4: The normalized invariant mass distribution of the Higgs boson pair for $PP \to hh$ at the 14 TeV LHC. The solid black line represents the result for SM. The red dashed line represents the result for EWBG with $\delta_h = 1, \delta_t^+ = 0, \delta_t^- = 0.1$, and the green line represents the result for EWBG with $\delta_h = 1, \delta_t^+ = 0, \delta_t^- = 0$.

1. *Anomalous trilinear Higgs coupling*

An interesting approach is to test these new interactions at next-leading order (NLO) in the associated hZ production [58, 59]. The advantage of this method is that the measurement of the hZ production cross section will be precise as $\mathcal{O}(0.1\%) \sim \mathcal{O}(1\%)$ at future e^+e^- colliders [60, 61]. Although this test for new Higgs self interaction is indirect and may suffer from some theoretical uncertainties [58], it is still a good guide for the future e^+e^- collider to search for the shape of the Higgs potential and the mechanism of EW baryogenesis.

Firstly, we give the NLO $e^+e^- \to hZ$ cross section in the SM. Here, the NLO $e^+e^- \to hZ$ cross section is calculated in the on-mass-shell renormalization scheme [62] and includes both radiative corrections from weak and electromagnetic processes as

$$\sigma_{\rm NLO} = \sigma_{\rm Born} + \sigma_{\rm weak} + \sigma_{\rm EM}, \tag{38}$$

where $\sigma_{\rm Born}$ is the Born cross section at tree level, $\sigma_{\rm weak}$ is the weak correction, and $\sigma_{\rm EM}$ includes contributions from the virtual photon correction to the eeZ vertex and real initial state radiations. We calculate $\sigma_{\rm EM}$ in the phase space slicing approach as [63, 64]

$$\sigma_{\rm EM} = \sigma_{\rm vir} + \sigma_{\rm soft} + \sigma_{\rm coll} + \sigma_{\rm finite}, \tag{39}$$

where $\sigma_{\rm vir}$ is the virtual correction, $\sigma_{\rm soft}$ describes the contribution of the soft photon emissions with the energy $E_\gamma < \Delta E$, $\sigma_{\rm coll}$ contains the contribution of photons collinear to the beam line with $E_\gamma > \Delta E$ and $\sin\theta_\gamma < \sin(\Delta\theta)$, and $\sigma_{\rm finite}$ includes the remaining correction from the hard photons with $E_\gamma > \Delta E$ and $\sin\theta_\gamma > \sin(\Delta\theta)$. $\sigma_{\rm NLO}$ would not depend on the two cut parameters ΔE and $\Delta\theta$, which are introduced to divide the phase space. Here we do not consider the contribution from real photons beyond $\mathcal{O}(\alpha)$, which may be important near the threshold region with $\sqrt{s} \sim m_h + m_Z$ [64].

We use the packages `FeynArts` [65], `FormCalc` [66], and `LoopTools` [67] to calculate NLO corrections. Fig. 5 shows the NLO $e^+e^- \to hZ$ cross section σ_{hZ} in the SM. Detailed investigations can be found in Refs. [68, 69]. It can be seen that the full NLO correction at $\sqrt{s} = 250$ GeV reduce σ_{hZ} by a factor of ~ 0.1.

In general, the hZZ coupling and σ_{hZ} could be modified by the anomalous Higgs trilinear coupling, anomalous top quark Yukawa coupling, and even other additional operators in new physics. The generic discussions can be found in Ref. [58]. The deviation of σ_{hZ} can be defined as

$$\delta_\sigma = \frac{\sigma_{hZ}}{\sigma_{hZ}^{\rm SM}} - 1. \tag{40}$$

At the CEPC with $\sqrt{s} = 240$ GeV, the contribution to δ_σ given by the anomalous Higgs trilinear coupling is much larger than that given by the anomalous top quark Yukawa coupling [70]. The UV divergences related to δ_h from different diagrams are automatically canceled. Assuming $\delta_t^\pm = 0$, δ_σ is given as a function of δ_h in Fig. 6. We can see that δ_σ is approximately proportional to δ_h as $\delta_\sigma \simeq 1.6\delta_h\%$ at $\sqrt{s} = 240$ GeV. For the future CEPC with an integrated luminosity of 10 ab^{-1}, the precision of σ_{zh} can be 0.4% [71]. Therefore, it is possible to test $|\delta_h| \sim 25\%$. In our EW baryogenesis scenario with sufficient SFOPT, $\delta_h \in (0.6, 1.5)$, which is well within the precision of CEPC.

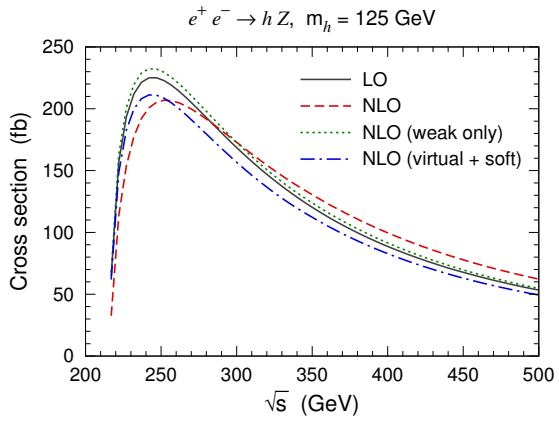

FIG. 5: The cross section of $e^+e^- \to hZ$ in the SM. Four lines denote cross sections at LO (solid), NLO (dashed), NLO without the electromagnetic corrections to the eeZ vertex (dot), and NLO with the real corrections only from the soft photons (dot-dashed), respectively. In the last case, we require the photon energy $E_\gamma < 0.1\sqrt{s}$, as in Refs. [59, 69].

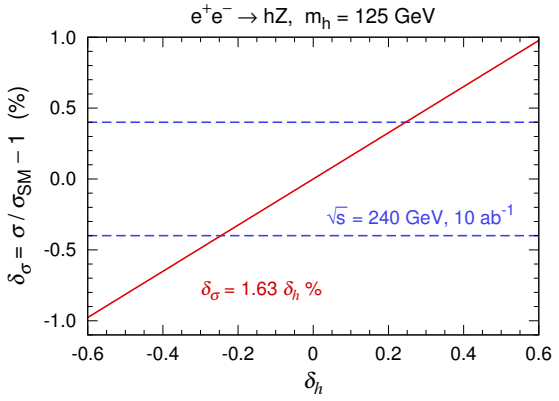

FIG. 6: The modification of the $e^+e^- \to hZ$ cross section as a function of the anomalous trilinear coupling δ_h (solid line) at the CEPC with $\sqrt{s} = 240$ GeV. The dashed lines denote the sensitivity to δ_σ for an integrated luminosity of 10 ab^{-1}.

2. *Anomalous top Yukawa coupling*

In this subsection, we investigate the effect of the anomalous top quark Yukawa coupling. In general, the scattering amplitude describing interactions between the Higgs and gauge bosons can be parameterized by [37]

$$A(hVV) = \frac{1}{v}(g_0 m_V^2 \epsilon_1 \epsilon_2 + g^+ f_{\mu\nu} f^{\mu\nu} + g^- f_{\mu\nu}, \tilde{f}^{\mu\nu}), \tag{41}$$

where $f^{\mu\nu} = \epsilon^\mu q^\nu - \epsilon^\nu q^\mu$ is the field strength with the polarization vector ϵ and momentum q, and $\tilde{f}^{\mu\nu} = \frac{1}{2}\epsilon^{\mu\nu\alpha\beta} f_{\alpha\beta}$ is the dual field strength tensor. The anomalous top quark Yukawa couplings enter the hZZ and $hZ\gamma$ vertices and the Higgs wavefunction counter term as shown in Fig. 7, and contribute to the g^+ and g^- terms in Eq. (41). The NLO correction comes from the interference between the g_0 term at tree level and the g^+ and g^- terms at one loop level.

We find that the interference term between the tree level amplitude and the amplitude contributed by the CP-odd top quark Yukawa coupling δ_t^- vanishes. Therefore this CP-odd coupling does not affect σ_{hz} at NLO. In principle, it will contribute to σ_{hz} at NNLO with a suppression factor of $\sim (\alpha/4\pi)^2$, but this contribution would be very small and beyond the CEPC sensitivity. Nonetheless, the anomalous CP-even top quark Yukawa coupling δ_t^+ can alter σ_{hz} at NLO. The vertex corrections introduce a divergence $\propto \delta_t^+$, which is canceled by the divergence $\propto \delta_t^+$ from the Higgs wave function counter terms in Fig. 7(b). We treat the counter terms that are proportional to $(\delta_t^+)^2$ as higher order contributions and do not include them in the calculation.

In Fig. 8, we show the cross section deviation δ_σ as a function of δ_t^+ at $\sqrt{s} = 240$ GeV, assuming $\delta_h = 0$. We find

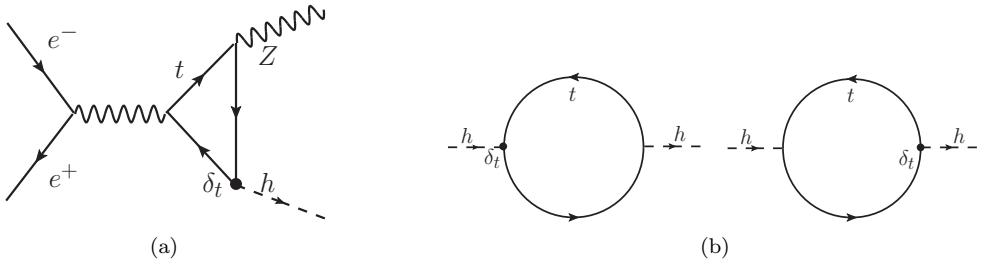

FIG. 7: Feynman diagrams describing NLO corrections to $e^+e^- \to hZ$ from the anomalous top quark Yukawa interaction, including the corrections to the $hZ\gamma$ and hZZ vertices (a) and to the Higgs wave function (b).

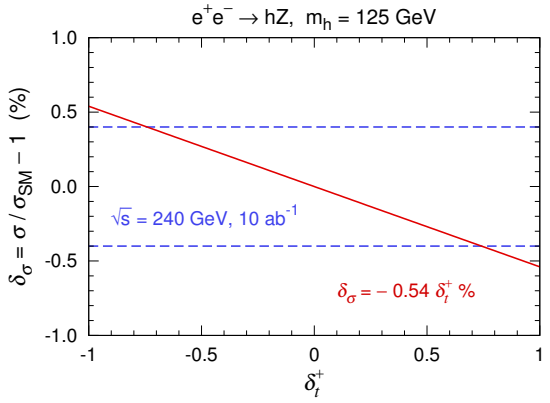

FIG. 8: The modification of the $e^+e^- \to hZ$ cross section as a function of the anomalous CP-even top quark Yukawa coupling δ_t^+ (solid line) at the CEPC with $\sqrt{s} = 240$ GeV. The dashed lines denote the sensitivity to δ_σ for an integrated luminosity of 10 ab^{-1}.

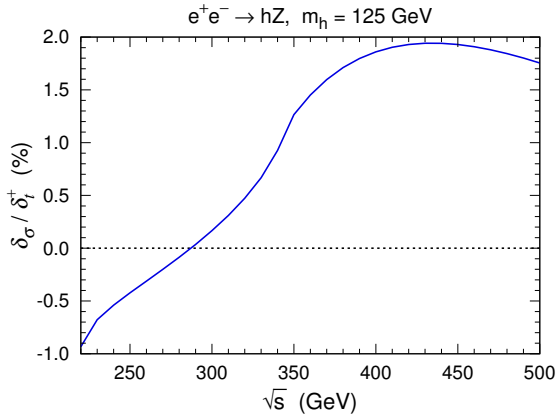

FIG. 9: δ_σ/δ_t^+ as a function of $\sqrt{s}$ for the $e^+e^- \to hZ$ process.

that $\delta_\sigma \simeq -0.54\delta_t^+\%$. If σ_{hz} can be determined to an accuracy of 0.4%, the anomalous coupling would be limited to be $|\delta_t^+| \lesssim 74\%$. We also give the energy dependence of δ_σ/δ_t^+ in Fig. 9. We can see that δ_σ/δ_t^+ increases with $\sqrt{s}$. At a collider with $\sqrt{s} = 500$ GeV, such as ILC, $\delta_\sigma \simeq 1.8\delta_t^+\%$. Then it is possible to determine $|\delta_t^+|$ down to $\sim 56\%$ with a σ_{hz} accuracy of 1% in this indirect approach. If we also let δ_h free, δ_σ at the CEPC would vary in the δ_t^+-δ_h plane as demonstrated in Fig. 10. The anomalous couplings would be constrained within the two black solid lines if a data set of 10 ab^{-1} is collected.

The anomalous top quark Yukawa coupling would also modify the Higgs couplings to gg and $\gamma\gamma$. Therefore, the precise measurements of the Higgs partial decay widths could set limits on δ_t^+ and δ_t^-. The deviation of a specified

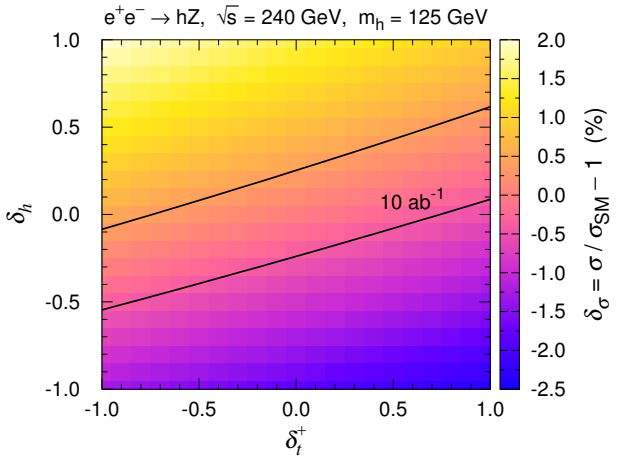

FIG. 10: The modification of the $e^+e^- \to hZ$ cross section in the δ_t^+-δ_h plane at the CEPC with $\sqrt{s} = 240$ GeV. The sold lines denote the sensitivity to δ_σ for an integrated luminosity of 10 ab^{-1}.

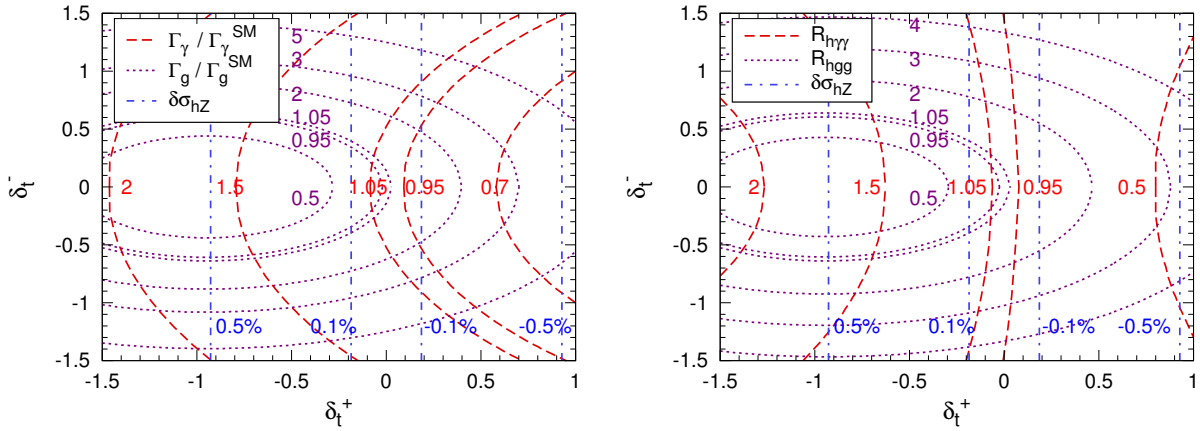

(a) (b)

FIG. 11: (a) Contours of δ_σ (dot-dashed), $\Gamma_{hgg}/\Gamma_{hgg}^{\rm SM}$ (dotted), and $\Gamma_{h\gamma\gamma}/\Gamma_{h\gamma\gamma}^{\rm SM}$ (dashed) in the δ_t^+-δ_t^- plane. (b) Contours of δ_σ (dot-dashed), R_{hgg} (dotted), and $R_{h\gamma\gamma}$ (dashed) in the δ_t^+-δ_t^- plane.

Higgs decay width Γ_{hXX} can be described by the signal strength

$$R_{hXX} = \frac{\sigma_{hZ} \cdot {\rm Br}(h \to XX)}{[\sigma_{hZ} \cdot {\rm Br}(h \to XX)]^{\rm SM}} = \frac{\sigma_{hZ}}{\sigma_{hZ}^{\rm SM}} \frac{\Gamma_{hXX}}{\Gamma_{hXX}^{\rm SM}} \frac{\Gamma_{\rm tot}^{\rm SM}}{\Gamma_{\rm tot}}, \tag{42}$$

where σ_h is the Higgs production cross section, and $\Gamma_{\rm tot}$ is the total Higgs decay width. At the CEPC with an integrated luminosity of 5 ab^{-1}, it is possible to determine R_{hgg} and $R_{h\gamma\gamma}$ up to precisions of $\sim 1.6\%$ and $\sim 9\%$, respectively [15]. In Fig. 11, we show $\Gamma_{hgg}/\Gamma_{hgg}^{\rm SM}$, $\Gamma_{h\gamma\gamma}/\Gamma_{h\gamma\gamma}^{\rm SM}$, R_{hgg}, $R_{h\gamma\gamma}$, and δ_σ in the δ_t^+-δ_t^- plane, assuming $\delta_h = 0$. We can see that Higgs decay measurements with an accuracy of 5% will set stringent limits on the anomalous top quark Yukawa couplings up to $\mathcal{O}(10\%)$.

IV. RENORMALIZABLE MODELS

The dimension-6 operators in Eq. (3) can be induced from certain renormalizable extensions of the SM. In this section we shall demonstrate a class of realistic models with vector-like quarks and a triplet Higgs.

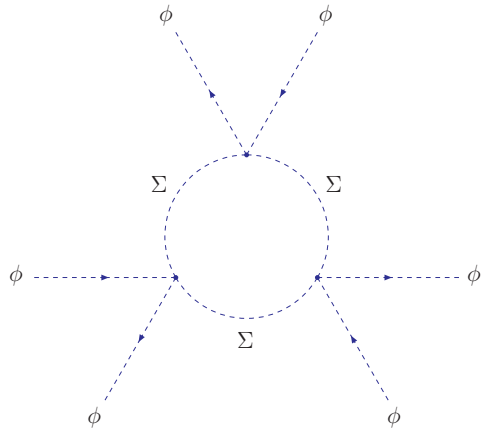

FIG. 12: One-loop diagram mediated by the Higgs triplet Σ without hypercharge for generating the dimension-6 coupling of the Higgs doublet ϕ.

A. The models with an $[SU(2)_L]$-triplet Higgs without hypercharge

We first consider the models with an $[SU(2)_L]$-triplet Higgs scalar with a zero hypercharge,

$$\Sigma(1,3,0) \;=\; \begin{bmatrix} \frac{1}{\sqrt{2}}\sigma^0 & \sigma^+ \\ \sigma^- & -\frac{1}{\sqrt{2}}\sigma^0 \end{bmatrix} = \Sigma^\dagger \,. \tag{43}$$

The Lagrangian involving the Higgs triplet Σ should be

$$\begin{aligned} \delta\mathcal{L} \;=\; & -\xi_\Sigma(\phi^T i\tau_2 \Sigma\tilde{\phi} + \text{H.c.}) + \frac{1}{2}\text{Tr}[(D^\mu\Sigma)^\dagger D_\mu\Sigma] \\ & -\frac{1}{2}M_\Sigma^2\text{Tr}(\Sigma^2) - \frac{1}{4}\zeta_\Sigma[\text{Tr}(\Sigma^2)]^2 - \frac{1}{2}\kappa_\Sigma\phi^\dagger\phi\text{Tr}(\Sigma^2)\,, \end{aligned} \tag{44}$$

where the covariant derivative is given by

$$D_\mu\Sigma \;=\; \partial_\mu\Sigma - ig\left[\frac{\tau_a}{2}W_\mu^a, \Sigma\right] . \tag{45}$$

Before the EW symmetry breaking, the Higgs triplet Σ can mediate a one-loop diagram as shown in Fig. 12 to induce the dimension-6 coupling of the SM Higgs doublet ϕ,

$$\mathcal{L} \;\supset\; -\frac{1}{\Lambda_\Sigma^2}(\phi^\dagger\phi)^3 \quad \text{with} \quad \Lambda_\Sigma = \frac{4\sqrt{2}\pi}{\kappa_\Sigma\sqrt{\kappa_\Sigma}}M_\Sigma \,. \tag{46}$$

For a proper choice of the parameters M_Σ and κ_Σ, we can fulfill the requirements of the cutoff scale Λ in the previous discussion. For example, we can take

$$M_\Sigma = 500\,\text{GeV} \quad \text{and} \quad \kappa_\Sigma = 5 \quad \Rightarrow \quad \Lambda_\Sigma \simeq 795\,\text{GeV} \,. \tag{47}$$

In order to generate the first term in Eq. (3), we further introduce two $[SU(2)_L]$-triplet quarks with the hypercharge $\pm 2/3$,

$$\begin{aligned} T_{L1}(3,3,+\tfrac{2}{3}) \;&=\; \begin{bmatrix} \frac{1}{\sqrt{2}}T_{L1}^{+\frac{2}{3}} & T_{L1}^{+\frac{5}{3}} \\ T_{L1}^{-\frac{1}{3}} & -\frac{1}{\sqrt{2}}T_{L1}^{+\frac{2}{3}} \end{bmatrix} , \\ T'_{L1}(3,3,-\tfrac{2}{3}) \;&=\; \begin{bmatrix} \frac{1}{\sqrt{2}}T_{L1}^{\prime-\frac{2}{3}} & T_{L1}^{\prime-\frac{5}{3}} \\ T_{L1}^{\prime+\frac{1}{3}} & -\frac{1}{\sqrt{2}}T_{L1}^{\prime-\frac{2}{3}} \end{bmatrix} , \end{aligned} \tag{48}$$

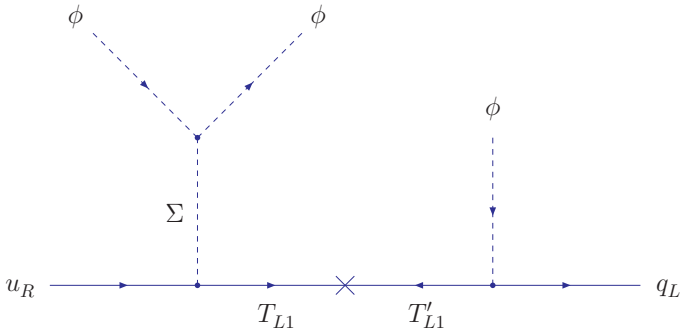

FIG. 13: Tree-level diagram mediated by the Higgs triplet Σ and the vector-like quark $T1 = T_{L1} + T'^c_{L1}$ for generating the dimension-6 couplings of the Higgs doublet ϕ to the left-handed quarks q_L and the right-handed up-type quarks u_R.

which have the Yukawa and mass terms as below,

$$\begin{aligned}\delta\mathcal{L} \supset & -f'_{1i}\bar{q}^c_{Li}i\tau_2 T'_{L1}\tilde{\phi} - f_{1j}\mathrm{Tr}(\overline{T}_{L1}\Sigma)u_{Rj} + \mathrm{H.c.} \\ & -M_{T1}[\mathrm{Tr}(i\tau_2\overline{T}'^c_{L1}i\tau_2 T_{L1}) + \mathrm{H.c.}]\,. \end{aligned} \tag{49}$$

We then can obtain the vector-like quark,

$$T1 = T_{L1} + T'^c_{L1}\,. \tag{50}$$

The vector-like quark $T1$ together with the Higgs triplet Σ can mediate the dimension-6 couplings of the Higgs doublet ϕ to the left-handed quarks q_L and the right-handed up-type quarks u_R at tree level,

$$\mathcal{L} \supset -\frac{f'^*_{1i}f_{1j}\xi_\Sigma}{M_{T1}M^2_\Sigma}\bar{q}_{Li}\tilde{\phi}u_{Rj}\phi^\dagger\phi + \mathrm{H.c.}\,. \tag{51}$$

The relevant diagram is shown in Fig. 13.

Alternatively, the first term in Eq. (3) can be induced by introducing two $[SU(2)_L]$-doublet quarks with the hypercharge $\pm 1/6$,

$$\begin{aligned} D_{L1}(3,2,+\tfrac{1}{6}) &= \begin{bmatrix} D_{L1}^{+\frac{2}{3}} \\ D_{L1}^{-\frac{1}{3}} \end{bmatrix}, \\ D'_{L1}(3,2,-\tfrac{1}{6}) &= \begin{bmatrix} D_{L1}^{\prime+\frac{1}{3}} \\ D_{L1}^{\prime-\frac{2}{3}} \end{bmatrix}, \end{aligned} \tag{52}$$

which have the following Yukawa and mass terms,

$$\begin{aligned}\delta\mathcal{L} \supset & -f'_{1i}\bar{q}^c_{Li}i\tau_2\Sigma D'_{L1} - f_{1j}\overline{D}_{L1}\phi u_{Rj} + \mathrm{H.c.} \\ & -M_{D1}(\overline{D}'^c_{L1}i\tau_2 D_{L1} + \mathrm{H.c.})\,. \end{aligned} \tag{53}$$

As shown in Fig. 14, by integrating out the vector-like quark,

$$D1 = D_{L1} + D'^c_{L1}\,, \tag{54}$$

and the Higgs triplet Σ, we can obtain the expected dimension-6 operator,

$$\mathcal{L} \supset -\frac{f'^*_{1i}f_{1j}\xi_\Sigma}{M_{D1}M^2_\Sigma}\bar{q}_{Li}\phi u_{Rj}\phi^\dagger\phi + \mathrm{H.c.}\,. \tag{55}$$

Note after the SM Higgs doublet ϕ develops its vev,

$$\langle\phi\rangle = \begin{bmatrix} \langle\phi^0\rangle \\ 0 \end{bmatrix}, \tag{56}$$

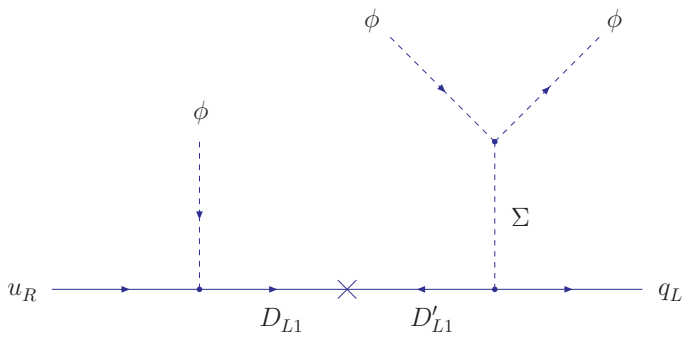

FIG. 14: Tree-level diagram mediated by the Higgs triplet Σ and the vector-like quark $D1 = D_{L1} + D'^{c}_{L1}$ for generating the dimension-6 couplings of the Higgs doublet ϕ to the left-handed quarks q_L and the right-handed up-type quarks u_R.

to drive the EW symmetry breaking, the Higgs triplet Σ will acquire an induced vev,

$$\langle\Sigma\rangle \;=\; \begin{bmatrix} \frac{1}{\sqrt{2}}\langle\sigma^0\rangle & 0 \\ 0 & -\frac{1}{\sqrt{2}}\langle\sigma^0\rangle \end{bmatrix} \;\text{ with}$$
$$\langle\sigma^0\rangle \simeq -\frac{\sqrt{2}\xi_\Sigma\langle\phi\rangle^2}{\overline{M}_\Sigma^2}\,,\;\; \overline{M}_\Sigma^2 = M_\Sigma^2 + \kappa_\Sigma\langle\phi\rangle^2\,. \tag{57}$$

Since the vev $\langle\Sigma\rangle$ is constrained by the ρ parameter,

$$\rho = 1 + \frac{2\langle\Sigma\rangle^2}{\langle\phi\rangle^2}\,, \tag{58}$$

it should be convenient to rewrite Eqs. (51) and (55) by

$$\mathcal{L} \;\supset\; \frac{f'^*_{1i} f_{1j}(M_\Sigma^2 + \kappa_\Sigma\langle\phi\rangle^2)\langle\Sigma\rangle}{\sqrt{2}M_{F1}M_\Sigma^2\langle\phi\rangle^2}\bar{q}_{Li}\phi u_{Rj}\phi^\dagger\phi + \text{H.c.}$$
$$\text{with}\;\; M_{F1} = M_{T1} \text{ or } M_{D1}\,. \tag{59}$$

Comparing with the above operators in Eq. (3), we can determine

$$x_u^{ij} = -\frac{16\sqrt{2}\pi^2 f'^*_{1i} f_{1j}(M_\Sigma^2 + \kappa_\Sigma\langle\phi\rangle^2)\langle\Sigma\rangle}{\kappa_\Sigma^3 M_{F1}\langle\phi\rangle^2}\,. \tag{60}$$

With the parameter choice (47), the CP violation for the EW baryogenesis can be satisfied,

$$x_u^{33} \simeq 0.74i\,, \tag{61}$$

by inputting

$$f'_{13} = if_{13} = \sqrt{4\pi}\,,\;\; f'_{11} = f'_{12} = f_{11} = f_{12} = 0\,,$$
$$M_{F1} = 800\,\text{GeV}\,,\;\; \langle\sigma^0\rangle = 2\,\text{GeV}\,,\;\; \langle\phi\rangle = 174\,\text{GeV}\,. \tag{62}$$

B. The models with an $[SU(2)_L]$-triplet Higgs with hypercharge

We now consider the models with an $[SU(2)_L]$-triplet Higgs scalar with a nonzero hypercharge,

$$\Delta(1,3,-1) \;=\; \begin{bmatrix} \frac{1}{\sqrt{2}}\delta^- & \delta^0 \\ \delta^{--} & -\frac{1}{\sqrt{2}}\delta^- \end{bmatrix}\,. \tag{63}$$

The scalar interactions of the SM then should be extended by

$$\delta\mathcal{L} \;=\; -\xi_\Delta(\tilde{\phi}^T i\tau_2\Delta\tilde{\phi} + \text{H.c.}) + \text{Tr}[(D^\mu\Delta)^\dagger D_\mu\Delta]$$

$$
\begin{aligned}
&-M_\Delta^2 \mathrm{Tr}(\Delta^\dagger\Delta) - \zeta_\Delta [\mathrm{Tr}(\Delta^\dagger\Delta)]^2 \\
&-\kappa_\Delta \phi^\dagger\phi \mathrm{Tr}(\Delta^\dagger\Delta)\,,
\end{aligned} \tag{64}
$$

with the covariant derivative,

$$
D_\mu \Delta \;=\; \partial_\mu \Delta - ig\left[\frac{\tau_a}{2} W_\mu^a, \Delta\right] + ig' B_\mu \Delta\,. \tag{65}
$$

Like the Higgs triplet without hypercharge Σ, the Higgs triplet with hypercharge Δ can also mediate a one-loop diagram to induce the expected dimension-6 interaction of the SM Higgs doublet ϕ,

$$
\mathcal{L} \;\supset\; -\frac{1}{\Lambda_\Delta}(\phi^\dagger\phi)^3 \;\;\text{with}\;\; \Lambda_\Delta = \frac{4\pi}{\kappa_\Delta\sqrt{\kappa_\Delta}} M_\Delta\,. \tag{66}
$$

Actually, we can easily obtain

$$
\Lambda_\Delta \simeq 785\,\mathrm{GeV} \;\;\text{for}\;\; M_\Delta = 500\,\mathrm{GeV}\,,\; \kappa_\Delta = 4\,. \tag{67}
$$

We also need two $[SU(2)_L]$-triplet quarks with the hypercharge $\pm 1/3$,

$$
\begin{aligned}
T_{L2}(3,3,-\tfrac{1}{3}) \;&=\; \begin{bmatrix} \frac{1}{\sqrt{2}} T_{L2}^{-\frac{1}{3}} & T_{L2}^{+\frac{2}{3}} \\ T_{L2}^{-\frac{4}{3}} & -\frac{1}{\sqrt{2}} T_{L2}^{-\frac{1}{3}} \end{bmatrix}, \\
T'_{L2}(3,3,+\tfrac{1}{3}) \;&=\; \begin{bmatrix} \frac{1}{\sqrt{2}} T_{L2}^{\prime+\frac{1}{3}} & T_{L2}^{\prime-\frac{2}{3}} \\ T_{L2}^{\prime+\frac{4}{3}} & -\frac{1}{\sqrt{2}} T_{L2}^{\prime-\frac{1}{3}} \end{bmatrix},
\end{aligned} \tag{68}
$$

which have the Yukawa and mass terms,

$$
\begin{aligned}
\delta\mathcal{L} \;\supset\; &-f'_{2i}\bar{q}^c_{Li} i\tau_2 T'_{L2}\phi - f_{2j}\mathrm{Tr}(\overline{T}_{L2}\Delta) u_{Rj} + \mathrm{H.c.} \\
&-M_{T2}[\mathrm{Tr}(i\tau_2 \overline{T}^{\prime c}_{L2} i\tau_2 T_{L2}) + \mathrm{H.c.}]\,,
\end{aligned} \tag{69}
$$

or two $[SU(2)_L]$-doublet quarks with the hypercharge $\pm\frac{7}{6}$,

$$
\begin{aligned}
D_{L2}(3,3,+\tfrac{7}{6}) \;&=\; \begin{bmatrix} D_{L2}^{+\frac{5}{3}} \\ D_{L2}^{-\frac{2}{3}} \end{bmatrix}, \\
D'_{L2}(3,3,-\tfrac{7}{6}) \;&=\; \begin{bmatrix} D_{L2}^{\prime-\frac{2}{3}} \\ D_{L2}^{\prime+\frac{5}{3}} \end{bmatrix},
\end{aligned} \tag{70}
$$

which have the Yukawa and mass terms,

$$
\begin{aligned}
\delta\mathcal{L} \;\supset\; &-f'_{2i}\bar{q}^c_{Li} i\tau_2 \Delta^\dagger D'_{L2} - f_{2j}\overline{D}_{L2}\tilde{\phi} u_{Rj} + \mathrm{H.c.} \\
&-M_{D2}(\overline{D}^{\prime c}_{L2} i\tau_2 D_{L2} + \mathrm{H.c.})\,.
\end{aligned} \tag{71}
$$

By integrating out the Higgs triplet Δ and the vector-like quark,

$$
T2 = T_{L2} + T^{\prime c}_{L2} \;\;\text{or}\;\; D2 = D_{L2} + D^{\prime c}_{L2}\,, \tag{72}
$$

we can obtain the following dimension-6 operator,

$$
\begin{aligned}
\delta\mathcal{L} \;\supset\; &-x_u^{ij}\frac{\phi^\dagger\phi}{\Lambda_\Delta^2}\bar{q}_{Li}\phi u_{Rj} + \mathrm{H.c.} \;\;\text{with} \\
&x_u^{ij} = -\frac{16\pi^2 f^{\prime *}_{1i} f_{1j}(M_\Delta^2 + \kappa_\Delta\langle\phi\rangle^2)\langle\Delta\rangle}{\kappa_\Delta^3 M_{F2}\langle\phi\rangle^2}\,, \\
&M_{F2} = M_{T2} \text{ or } M_{D2}\,.
\end{aligned} \tag{73}
$$

In the presence of the parameter choice (67), a desirable CP violation can be

$$\begin{aligned} & x_u^{33} = 0.95i \ \text{ for} \\ & f'_{13} = if_{13} = \sqrt{4\pi}\,,\ f'_{11} = f'_{12} = f_{11} = f_{12} = 0\,, \\ & M_{F2} = 800\,\text{GeV}\,,\ \langle\Delta\rangle = 2\,\text{GeV}\,,\ \langle\phi\rangle = 174\,\text{GeV}\,. \end{aligned} \tag{74}$$

It should be noted like the vev $\langle\Sigma\rangle$, the vev $\langle\Delta\rangle$ which is given by

$$\begin{aligned} \langle\Delta\rangle \ &= \ \begin{bmatrix} 0 & \langle\delta^0\rangle \\ 0 & 0 \end{bmatrix} \ \text{ with} \\ & \langle\delta^0\rangle \simeq -\frac{\xi_\Delta\langle\phi\rangle^2}{\overline{M}_\Delta^2}\,,\ \ \overline{M}_\Delta^2 = M_\Delta^2 + \kappa_\Delta\langle\phi\rangle^2\,, \end{aligned} \tag{75}$$

is also constrained by the ρ parameter,

$$\rho = 1 + \frac{2\langle\Delta\rangle^2}{\langle\phi\rangle^2 + 2\langle\Delta\rangle^2}\,. \tag{76}$$

Furthermore, the Higgs triplet Δ can have the Yukawa couplings with the SM left-handed leptons,

$$\delta\mathcal{L} \supset -y\bar{l}_L^c i\tau_2\Delta^\dagger l_L + \text{H.c.} \ \text{ with } \ \ l_L(1,2,-\tfrac{1}{2}) \ = \begin{bmatrix} \nu_L \\ e_L \end{bmatrix}. \tag{77}$$

Due to the small neutrino masses, the Yukawa couplings f should be tiny when the vev $\langle\Delta\rangle$ is expected at the GeV scale. To avoid this fine tuning, we can arrange the Higgs triplet Δ for a zero lepton number to forbid the above Yukawa couplings if the lepton number is exactly conserved or is only softly broken.

V. CONCLUSION

Unravelling the true shape of the Higgs potential, the type of the phase transition and the EW baryogenesis is the central issue after the discovery of the Higgs boson, and is a major goal for the future CEPC. We have investigated the simple extension of the Higgs sector by introducing the dimensions-6 operators $-x_u^{ij}\frac{\phi^\dagger\phi}{\Lambda^2}\bar{q}_{Li}\tilde{\phi}u_{Rj} + \text{H.c.} - \frac{\kappa}{\Lambda^2}(\phi^\dagger\phi)^3$ using the EFT and discussed how to test this scenario at colliders. We have found that the $\frac{\kappa}{\Lambda^2}(\phi^\dagger\phi)^3$ operator could provide another possible Higgs potential with the same Higgs mass and vev, easily realize the SFOPT, and modify the trilinear Higgs boson coupling obviously. The sizable CP violation source can be supplied by the operator $-x_u^{ij}\frac{\phi^\dagger\phi}{\Lambda^2}\bar{q}_{Li}\tilde{\phi}u_{Rj} + \text{H.c.}$, which can induce the anomalous top quark Yukawa coupling. Both the anomalous trilinear Higgs boson coupling and the anomalous top quark Yukawa coupling can make contributions to the Higgs boson pair production at the LHC, and the analytical expressions and the simple numerical results are given in this paper. The invariant mass distribution of Higgs boson pair at the LHC is expected to be different from the SM prediction to achieve SFOPT and EW baryogenesis. However, due to the precision limit of the LHC, the CEPC is needed to precisely test this scenario, and the anomalous coupling can be tested indirectly from the precise measurements of the Zh production at the CEPC. Besides the investigation using the EFT to get the model independent predictions, concrete renormalizable models are built, and they can give the concerned dimension-6 operators. The study will help us to understand the nature of EW symmetry breaking and the origin of BAU from the current LHC experiments and the future CEPC experiments.

Acknowledgments

We thank Xiao-Jun Bi for early cooperation and useful discussion. F.P.H. and X.Z. are supported by the NSFC under grants Nos. 11121092, 11033005, 11375220 and also by the CAS pilotB program. P.H.G. is supported by the Shanghai Jiao Tong University under Grant No. WF220407201, the Recruitment Program for Young Professionals under Grant No. 15Z127060004, the Shanghai Laboratory for Particle Physics and Cosmology under Grant No. 11DZ2260700. P.F.Y. and Z.H.Y. are supported by the NSFC under grants No. 11475189. Z.H.Y. is also supported by the Australian Research Council.

VI. APPENDIX

The scalar integrals are defined as:

$$C_{ij} = \int \frac{d^4q}{i\pi^2} \frac{1}{(q^2-m_t^2)((q+p_i)^2-m_t^2)((q+p_i+p_j)^2-m_t^2)}, \tag{78}$$

$$D_{ijk} = \int \frac{d^4q}{i\pi^2} \frac{1}{(q^2-m_t^2)((q+p_i)^2-m_t^2)((q+p_i+p_j)^2-m_t^2)((q+p_i+p_j+p_k)^2-m_t^2)}. \tag{79}$$

The analytic expressions can be found in Ref. [72].

[1] P. A. R. Ade *et al.* [Planck Collaboration], Astron. Astrophys. **571**, A16 (2014) [arXiv:1303.5076 [astro-ph.CO]].
[2] K. A. Olive *et al.* [Particle Data Group Collaboration], Chin. Phys. C **38**, 090001 (2014).
[3] A. D. Sakharov, Pisma Zh. Eksp. Teor. Fiz. **5**, 32 (1967) [JETP Lett. **5**, 24 (1967)] [Sov. Phys. Usp. **34**, 392 (1991)] [Usp. Fiz. Nauk **161**, 61 (1991)].
[4] M. Dine and A. Kusenko, Rev. Mod. Phys. **76**, 1 (2003) [hep-ph/0303065].
[5] G. Aad *et al.* [ATLAS Collaboration], Phys. Lett. B **716**, 1 (2012) [arXiv:1207.7214 [hep-ex]].
[6] S. Chatrchyan *et al.* [CMS Collaboration], Phys. Lett. B **716**, 30 (2012) [arXiv:1207.7235 [hep-ex]].
[7] V. A. Kuzmin, V. A. Rubakov and M. E. Shaposhnikov, Phys. Lett. B **155**, 36 (1985).
[8] M. Trodden, Rev. Mod. Phys. **71**, 1463 (1999) [hep-ph/9803479].
[9] D. E. Morrissey and M. J. Ramsey-Musolf, New J. Phys. **14**, 125003 (2012) [arXiv:1206.2942 [hep-ph]].
[10] X. m. Zhang, Phys. Rev. D **47**, 3065 (1993) [hep-ph/9301277].
[11] X. Zhang and B. L. Young, Phys. Rev. D **49**, 563 (1994) [hep-ph/9309269].
[12] K. Whisnant, B. L. Young and X. Zhang, Phys. Rev. D **52**, 3115 (1995) [hep-ph/9410369].
[13] X. Zhang, S. K. Lee, K. Whisnant and B. L. Young, Phys. Rev. D **50**, 7042 (1994) [hep-ph/9407259].
[14] F. P. Huang and C. S. Li, Phys. Rev. D **92**, 075014 (2015) [arXiv:1507.08168 [hep-ph]].
[15] [CEPC-SPPC Study Group Collaboration], IHEP-CEPC-DR-2015-01, IHEP-TH-2015-01, HEP-EP-2015-01.
[16] C. Grojean, G. Servant and J. D. Wells, Phys. Rev. D **71**, 036001 (2005) [hep-ph/0407019].
[17] C. Delaunay, C. Grojean and J. D. Wells, JHEP **0804**, 029 (2008) [arXiv:0711.2511 [hep-ph]].
[18] B. Grinstein and M. Trott, Phys. Rev. D **78**, 075022 (2008) [arXiv:0806.1971 [hep-ph]].
[19] D. J. H. Chung, A. J. Long and L. T. Wang, Phys. Rev. D **87**, no. 2, 023509 (2013) [arXiv:1209.1819 [hep-ph]].
[20] S. W. Ham and S. K. Oh, Phys. Rev. D **70**, 093007 (2004) [hep-ph/0408324].
[21] D. Bodeker, L. Fromme, S. J. Huber and M. Seniuch, JHEP **0502**, 026 (2005) [hep-ph/0412366].
[22] D. Y.-J. Chu, K. Jansen, B. Knippschild, C.-J. D. Lin and A. Nagy, Phys. Lett. B **744**, 146 (2015) doi:10.1016/j.physletb.2015.03.050 [arXiv:1501.05440 [hep-lat]].
[23] F. P. Huang, Y. Wan, D. G. Wang, Y. F. Cai and X. Zhang, arXiv:1601.01640 [hep-ph].
[24] M. Quiros, hep-ph/9901312.
[25] L. Dolan and R. Jackiw, Phys. Rev. D **9**, 3320 (1974).
[26] A. Noble and M. Perelstein, Phys. Rev. D **78**, 063518 (2008) doi:10.1103/PhysRevD.78.063518 [arXiv:0711.3018 [hep-ph]].
[27] A. Katz and M. Perelstein, JHEP **1407**, 108 (2014) doi:10.1007/JHEP07(2014)108 [arXiv:1401.1827 [hep-ph]].
[28] D. Curtin, P. Meade and C. T. Yu, JHEP **1411**, 127 (2014) doi:10.1007/JHEP11(2014)127 [arXiv:1409.0005 [hep-ph]].
[29] O. Lebedev, Phys. Lett. B **697**, 58 (2011) doi:10.1016/j.physletb.2011.01.048 [arXiv:1011.2630 [hep-ph]].
[30] S. J. Huber, M. Pospelov and A. Ritz, Phys. Rev. D **75**, 036006 (2007) doi:10.1103/PhysRevD.75.036006 [hep-ph/0610003].
[31] J. R. Espinosa, B. Gripaios, T. Konstandin and F. Riva, JCAP **1201**, 012 (2012) [arXiv:1110.2876 [hep-ph]].
[32] J. M. Cline and K. Kainulainen, JCAP **1301**, 012 (2013) doi:10.1088/1475-7516/2013/01/012 [arXiv:1210.4196 [hep-ph]].
[33] L. Fromme and S. J. Huber, JHEP **0703**, 049 (2007) doi:10.1088/1126-6708/2007/03/049 [hep-ph/0604159].
[34] J. M. Cline, K. Kainulainen and M. Trott, JHEP **1111**, 089 (2011) doi:10.1007/JHEP11(2011)089 [arXiv:1107.3559 [hep-ph]].
[35] J. Shu and Y. Zhang, Phys. Rev. Lett. **111**, no. 9, 091801 (2013) [arXiv:1304.0773 [hep-ph]].
[36] J. Brod, U. Haisch and J. Zupan, JHEP **1311**, 180 (2013) [arXiv:1310.1385 [hep-ph], arXiv:1310.1385].
[37] S. Inoue, M. J. Ramsey-Musolf and Y. Zhang, Phys. Rev. D **89**, 115023 (2014) [arXiv:1403.4257 [hep-ph]].
[38] Y.-T. Chien, V. Cirigliano, W. Dekens, J. de Vries and E. Mereghetti, arXiv:1510.00725 [hep-ph].
[39] J. Baron *et al.* [ACME Collaboration], Science **343**, 269 (2014) doi:10.1126/science.1248213 [arXiv:1310.7534 [physics.atom-ph]].
[40] L. Bian, T. Liu and J. Shu, Phys. Rev. Lett. **115**, 021801 (2015) doi:10.1103/PhysRevLett.115.021801 [arXiv:1411.6695 [hep-ph]].
[41] K. Fuyuto, J. Hisano and E. Senaha, arXiv:1510.04485 [hep-ph].
[42] K. Nishiwaki, S. Niyogi and A. Shivaji, JHEP **1404**, 011 (2014) [arXiv:1309.6907 [hep-ph]].
[43] S. Khatibi and M. M. Najafabadi, Phys. Rev. D **90**, no. 7, 074014 (2014) [arXiv:1409.6553 [hep-ph]].

[44] N. Liu, S. Hu, B. Yang and J. Han, JHEP **1501**, 008 (2015) [arXiv:1408.4191 [hep-ph]].
[45] R. Mertig, M. Bohm and A. Denner, Comput. Phys. Commun. **64**, 345 (1991).
[46] V. Barger, L. L. Everett, C. B. Jackson and G. Shaughnessy, Phys. Lett. B **728**, 433 (2014) [arXiv:1311.2931 [hep-ph]].
[47] D. Y. Shao, C. S. Li, H. T. Li and J. Wang, JHEP **1307**, 169 (2013) [arXiv:1301.1245 [hep-ph]].
[48] A. Papaefstathiou, L. L. Yang and J. Zurita, Phys. Rev. D **87**, no. 1, 011301 (2013) [arXiv:1209.1489 [hep-ph]].
[49] F. Goertz, A. Papaefstathiou, L. L. Yang and J. Zurita, JHEP **1306**, 016 (2013) [arXiv:1301.3492 [hep-ph]].
[50] C. R. Chen and I. Low, Phys. Rev. D **90**, no. 1, 013018 (2014) [arXiv:1405.7040 [hep-ph]].
[51] Q. Li, Z. Li, Q. S. Yan and X. Zhao, Phys. Rev. D **92**, no. 1, 014015 (2015) [arXiv:1503.07611 [hep-ph]].
[52] H. J. He, J. Ren and W. Yao, arXiv:1506.03302 [hep-ph].
[53] Q. H. Cao, Y. Liu and B. Yan, arXiv:1511.03311 [hep-ph].
[54] S. Dawson, A. Ismail and I. Low, Phys. Rev. D **91**, no. 11, 115008 (2015) doi:10.1103/PhysRevD.91.115008 [arXiv:1504.05596 [hep-ph]].
[55] P. Huang, A. Joglekar, B. Li and C. E. M. Wagner, arXiv:1512.00068 [hep-ph].
[56] E. W. N. Glover and J. J. van der Bij, Nucl. Phys. B **309**, 282 (1988).
[57] T. Plehn, M. Spira and P. M. Zerwas, Nucl. Phys. B **479**, 46 (1996) [Nucl. Phys. B **531**, 655 (1998)] [hep-ph/9603205].
[58] M. McCullough, Phys. Rev. D **90**, no. 1, 015001 (2014) [Phys. Rev. D **92**, no. 3, 039903 (2015)] [arXiv:1312.3322 [hep-ph]].
[59] C. Englert and M. McCullough, JHEP **1307**, 168 (2013) [arXiv:1303.1526 [hep-ph]].
[60] H. Baer, T. Barklow, K. Fujii, Y. Gao, A. Hoang, S. Kanemura, J. List and H. E. Logan *et al.*, arXiv:1306.6352 [hep-ph].
[61] P. Azzi, Nuovo Cim. C **037**, no. 02, 11 (2014).
[62] A. Denner, Fortsch. Phys. **41**, 307 (1993) [arXiv:0709.1075 [hep-ph]].
[63] M. Bohm and S. Dittmaier, Nucl. Phys. B **409**, 3 (1993).
[64] A. Denner, S. Dittmaier, M. Roth and M. M. Weber, Nucl. Phys. B **660**, 289 (2003) [hep-ph/0302198].
[65] T. Hahn, Comput. Phys. Commun. **140**, 418 (2001) [hep-ph/0012260].
[66] T. Hahn and M. Perez-Victoria, Comput. Phys. Commun. **118**, 153 (1999) [hep-ph/9807565].
[67] G. J. van Oldenborgh, Comput. Phys. Commun. **66**, 1 (1991).
[68] J. Fleischer and F. Jegerlehner, Nucl. Phys. B **216**, 469 (1983).
[69] A. Denner, J. Kublbeck, R. Mertig and M. Bohm, Z. Phys. C **56**, 261 (1992).
[70] C. Shen and S. h. Zhu, Phys. Rev. D **92**, 094001 (2015) [arXiv:1504.05626 [hep-ph]].
[71] M. Bicer *et al.* [TLEP Design Study Working Group Collaboration], JHEP **1401**, 164 (2014) [arXiv:1308.6176 [hep-ex]].
[72] R. K. Ellis and G. Zanderighi, JHEP **0802**, 002 (2008) [arXiv:0712.1851 [hep-ph]].